# Nonlinear Instability of Rayleigh-Taylor Waves Subjected to Time-Dependent Temperatures

Yusry O. El-Dib[a] and Yassmin D. Mahmoud[b]

[a] Department of Mathematics, Faculty of Education, Ain Shams University, Heliopolis, Cairo, Egypt
[b] Department of Mathematics, Faculty of Science, Suez Canal University, Ismailia, Egypt

Reprint requests to Dr. Y. D. M.; E-mail: jas-dess@hotmail.com

Z. Naturforsch. **63a,** 575 – 584 (2008); received February 22, 2008

The effect of time-dependent temperatures on surface waves is investigated. Nonlinear stability analysis is performed to describe waves propagating along the interface between two fluids in the presence of mass and heat transfer. Due to the presence of periodic forces, resonance interaction is balanced. The use of a multiple-scales method yields different nonlinear Schrödinger equations. Two parametric nonlinear Schrödinger equations are derived in resonance cases. One of these equations has not been treated before. Its stability criteria depending on linear perturbation are derived. A classical nonlinear Schrödinger equation is derived in the nonresonance case. Stability conditions are obtained analytically and investigated numerically. It is shown that the resonance point depends on the external frequency and that, for $\Omega \approx 2\omega$ and $\Omega \approx \omega$, where $\Omega$ and $\omega$ are the external and disturbance frequency, the external frequency has stabilizing and destabilizing effects, respectively.

*Key words:* Nonlinear Stability; Mass and Heat Transfer; Periodic Heat; Nonlinear Schrödinger Equation.

## 1. Introduction

Many transport processes exist in nature and in industrial applications in which the transfer of heat and mass occurs simultaneously as a result of combined buoyancy effects of thermal diffusion and diffusion of chemical species. In the last decade, intensive research efforts have been devoted to problems in heat and mass transfer in view of their application to astrophysics, geophysics and engineering. The phenomenon of heat and mass transfer also occurs in chemical processes such as food processing. In engineering applications, the concentration differences are created either by injecting foreign gases or by coating the surface with evaporating material due to the heat of the surface. In practice, hydrogen, helium, water-vapour, oxygen, ammonia etc., are foreign gases which are injected in the air-flowing past bodies.

When two fluids are divided by an interface, the interfacial stability is usually discussed neglecting heat and mass transfer across the interface. The mechanism of heat and mass transfer across an interface (e. g. gas-liquid interface) is of great importance in many environmental processes. These include boilers, condensers, evaporators, gas absorbers, pipelines, chemical reactors, nuclear reactors, and problems such as the aeration of rivers and seas. In most cases of practical importance the liquid is turbulent and transport across the gas-liquid interface is governed by the liquid side. As a result, the characteristics of turbulence in liquid flows near the interface are significant in understanding the transport across the gas-liquid interface.

Nowadays, a number of attempts are made to predict the heat and mass transfer coefficients at a gas-liquid interface theoretically and experimentally. Experimentally, Fortescue and Pearson [1] measured mass transfer coefficients for gas absorption in water tunnels, and Rashidi [2] in natural streams. In these researches, no measurements on the turbulence structure were made. Salazar and Marshall [3] and Komori et al. [4] measured a few turbulence characteristics by means of hot film velocimetry and optical methods. However, these investigations are not complete because of the difficulty of making accurate measurements of turbulence at and near free surfaces, and because the turbulence structure has not been clarified experimentally.

The effect of mass and heat transfer across the interface should be taken into account in stability discussions. However, with linear analysis, the stability criteria remain the same as in the case with neglect of heat and mass transfer across the interface. Hsieh [5] found that when the vapour region is hotter than the liquid region, as is usually, the effect of mass and heat transfer tends to inhibit the growth of instability. Korichi and Oufer [6] studied the heat transfer enhancement in an oscillating flow in a channel with periodical upper and lower walls. It is clear that such a uniform model based on a linear theory is inadequate to explain the mechanism involved, and a nonlinear theory is needed to reveal the effect of heat and mass transfer on the stability of the system. However, Hsieh [7, 8] formulated the general problem of interfacial fluid flow with mass and heat transfer; the model was then applied to stability analysis of both Rayleigh-Taylor and Kelvin-Helmholtz problems in film boiling and heat transfer. For the case of the Rayleigh-Taylor stability problem, Hsieh found that the simplified version retains the essential feature that, although the effect of mass and heat transfer tends to reduce the growth rate of instability, the criterion for stability is still the same as in the classical results. For this formulation, the effect of mass and heat transfer is revealed through a single parameter, $\alpha$. Thus, the correlation of experimental data would be greatly facilitated by these simplifications. Following Hsieh [5, 7, 8], Mohamed et al. [9, 10] and Elhefnawy and Moatimid [11] investigated the nonlinear electro-hydrodynamic Rayleigh-Taylor instability with mass and heat transfer.

Here we reinvestigate the Hsieh [8] problem for the nonlinear Rayleigh-Taylor instability, but in the presence of time-dependent mass and heat transfer. The temperature at the rigid boundaries is periodic in time.

The phenomenon of parametric resonance arises in many branches of physics and engineering. One of the important problems is the dynamic instability which is the response of mechanical and elastic systems to time-varying loads, especially periodic loads. There are cases in which the introduction of a small vibration loading can stabilize a system, which is statically unstable, or destabilize a system, that is statically stable. The treatment of the parametric excitation system having many degrees of freedom and distinct natural frequencies is usually operated by using the multiple time scales as given by Nayfeh [12]. The behaviour of such systems, in linear theory, is described by an equation of the Hill or Mathieu type [13, 14]. The effect of a periodic electric field with mass and heat transfer on the linear Rayleigh-Taylor instability was investigated by Moatimid [15]. He demonstrated that the coefficient of mass and heat transfer has a destabilizing effect.

In the nonlinear theory, the stability of parametric excitation is described by parametric nonlinear Schrödinger equations [16 – 20]. El-Dib [21] discussed the nonlinear interfacial instability of two superposed electrified fluids stressed by a periodic electric field. Based on the method of multiple scales, two nonlinear Schrödinger equations are derived in the nonresonance case. The necessary and sufficient conditions for stability are obtained. It is noted that the constant electric field plays a dual role in the stability analysis, and the field frequency changes the mechanism due to the dual role of the electric field. El-Dib [22] discussed the sub-harmonic response of two resonant modes of interfacial gravity-capillary waves between two electrified fluids of infinite depth under the influence of a constant horizontal electric field. Elhefnawy et al. [23] reinvestigated El-Dib's work [21] taking into account the effect of mass and heat transfer. Recently, Moatimid [24] investigated the stability of two rigidly rotating magnetic fluid columns in the presence of mass and heat transfer. His boundary-value problem leads to a transcendental differential equation. Therefore, the method of multiple scales is adopted to determine the stability conditions. In addition, the stability properties of ferromagnetic fluids in the presence of an oblique mass and heat transfer was investigated by Moatimid [25]. His analysis revealed the case of a uniform magnetic field as well as a periodic one. A most recent work on this topic was also introduced by Moatimid [26]. His system is composed of a streaming dielectric fluid sheet of finite thickness embedded between two different streaming finite dielectric fluids. The interface permits mass and heat transfer. His analysis revealed that the sheet thickness and mass and heat transfer parameters have a dual influence on the stability picture, especially at small values of the wavenumber. Mahmoud [27] studied the nonlinear Rayleigh-Taylor instability of two fluids with cylindrical interface under the effect of a periodic radial magnetic field. In all these studies, the frequency of the periodic electric field, the periodic magnetic field and the periodic acceleration have played a destabilizing influence on the nonlinear stability picture. In our current research, we found another role for the temperature frequency.

## 2. Basic Equations

The derivation of the dynamical system for time-dependent mass and heat transfer is presented in this section. A two-dimensional wave motion of inviscid fluids confined between two parallel planes at $y = -h_1$ and $y = h_2$ is performed. The fluids are homogeneous, incompressible and exhibit interfacial tension.

At equilibrium, the interfacial surface exhibits a plane at $y = 0$. The fluid of density $\rho^{(1)}$ occupies the region $-h_1 < y < 0$, and the fluid of density $\rho^{(2)}$ the region $0 > y > h_2$. Due to a small departure from equilibrium the interface is given by

$$S(x,t) = y - \eta(x,t) = 0. \tag{1}$$

The periodic temperatures at $y = h_2$, $y = -h_1$ and $y = 0$ are $\varepsilon T^{(2)} \cos \Omega t$, $\varepsilon T^{(1)} \cos \Omega t$ and $\varepsilon T^{(0)} \cos \Omega t$, respectively, where $\Omega$ is the external frequency and $\varepsilon$ is a small dimensionless parameter which measures the temperatures amplitude.

The motion is assumed to be irrotational; hence the basic equations governing the flow are

$$\nabla^2 \phi^{(1)} = 0, \tag{2}$$

$$\nabla^2 \phi^{(2)} = 0, \tag{3}$$

where $\phi$ is the velocity hydrostatic field potential. The velocity potential satisfies the conditions

$$\left(\frac{\partial \phi^{(1)}}{\partial y}\right)_{y=-h_1} = \left(\frac{\partial \phi^{(2)}}{\partial y}\right)_{y=h_2} = 0. \tag{4}$$

The interfacial conditions obtained from the conservation of mass and momentum are given by [7]

$$\rho^{(1)} \left(\frac{\partial S}{\partial t} + \nabla \phi^{(1)} \cdot \nabla S\right) = \rho^{(2)} \left(\frac{\partial S}{\partial t} + \nabla \phi^{(2)} \cdot \nabla S\right), \tag{5}$$

$$\begin{aligned} &\rho^{(1)}(\nabla \phi^{(1)} \cdot \nabla S) \left(\frac{\partial S}{\partial t} + \nabla \phi^{(1)} \cdot \nabla S\right) \\ &= \rho^{(2)}(\nabla \phi^{(2)} \cdot \nabla S) \left(\frac{\partial S}{\partial t} + \nabla \phi^{(2)} \cdot \nabla S\right) \\ &\quad + \left[P^{(2)} - P^{(1)} - \sigma \left(\frac{1}{R_1} + \frac{1}{R_2}\right)\right] |\nabla S|, \end{aligned} \tag{6}$$

where $\sigma$ is the surface tension coefficient, $R_1$ and $R_2$ are the two principal radii of curvature for the interface, and $P^{(1)}$ and $P^{(2)}$ are the hydrostatic pressure of the lower and upper fluids, respectively. The interfacial condition for energy transfer is given by

$$L\rho^{(1)} \left(\frac{\partial S}{\partial t} + \nabla \phi^{(1)} \cdot \nabla S\right) = F(\eta), \tag{7}$$

where $L$ is the latent heat released when the fluid is transformed from phase 1 to phase 2. The left-hand side of (7) represents the net flux from the interface into the fluid regions when such a phase transformation is present. This quantity is taken to be approximately expressible in terms of the balance of heat fluxes in the fluid regions if the system is instantaneously in dynamic equilibrium. Let us express $F(\eta)$ in terms of a power series expansion of $\eta$. We can rewrite (7) as

$$\rho^{(1)} \left(\frac{\partial S}{\partial t} + \nabla \phi^{(1)} \cdot \nabla S\right) = \alpha(\eta + \alpha_2 \eta^2 + \alpha_3 \eta^3). \tag{8}$$

The coefficients $\alpha$, $\alpha_2$ and $\alpha_3$ are given by

$$\begin{aligned} \alpha &= \varepsilon \alpha_0 \cos \Omega t, \\ \alpha_0 &= \frac{G}{L}\left(\frac{1}{h_1} + \frac{1}{h_2}\right), \\ \alpha_2 &= \frac{1}{h_2} - \frac{1}{h_1}, \\ \alpha_3 &= \frac{h_1^3 + h_2^3}{h_1^2 h_2^2 (h_1 + h_2)}, \\ G &= \frac{K^{(2)}(T^{(0)} - T^{(2)})}{h_2} = \frac{K^{(1)}(T^{(1)} - T^{(0)})}{h_1}, \end{aligned}$$

where $G$ is the equilibrium heat flux and $K^{(1)}$ and $K^{(2)}$ are the lower and upper thermal conductivities, respectively.

To suggest the nonlinear interactions of small but finite amplitude waves, we apply the method of multiple scales. Nayfeh [28] applied the same method to the classical Rayleigh-Taylor problem with two immiscible fluids. The perturbations in view of the method of multiple scales were used to perturb the nonlinear elevation and the periodic terms at the same time. The small parameter $\varepsilon$ was introduced in order to describe both outer and inner perturbations [21]. Thus, it is convenient to choose $\varepsilon$ as the amplitude of the temperatures $T^{(j)}$ ($j = 0, 1, 2$). The surface deflection $\eta(x,t)$ is expanded as a power series in $\varepsilon$ to indicate the outer perturbation in the following form:

$$\eta = \varepsilon \eta_1 + \varepsilon^2 \eta_2 + \varepsilon^3 \eta_3 + \dots . \tag{9}$$

Then every order of the above elevation will be perturbed in the form

$$\eta_n = \eta_{n0} + \varepsilon \eta_{n1} + \varepsilon^2 \eta_{n2} + \dots, \tag{10}$$

to indicate the inner perturbation. The perturbation of $\eta_n$ is expanded about $\eta_{n0}$, which represents the elevation in the absence of the temperatures. So, when we substitute (10) into (9), we obtain

$$\eta = \varepsilon\eta_{10} + \varepsilon^2(\eta_{20} + \eta_{11}) + \varepsilon^3(\eta_{30} + \eta_{21} + \eta_{12}) + \dots, \tag{11}$$

where $\varepsilon\eta_{10} + \varepsilon^2\eta_{20} + \varepsilon^3\eta_{30} + \dots$ represents the elevation obtained by Nayfeh [28] in the case of absence of mass and heat transfer.

To study the perturbation of the system, in view of the multiple-scales method [12], the variables $t$ and $x$ are scaled in the following manner:

$$X_n = \varepsilon^n x, \quad T_n = \varepsilon^n t, \quad n = 0,1,2, \tag{12}$$

where $\varepsilon$ represents a small parameter characterizing the steepness ratio of the wave as well as measuring the amplitude temperatures. The perturbation quantities $\eta$ and $\phi$ are expanded in the form

$$\eta(x,t) = \sum_{n=1}^{3} \varepsilon^n \eta_n(X_0,X_1,X_2;T_0,T_1,T_2) + o(\varepsilon^4), \tag{13}$$

$$\phi(x,t) = \sum_{n=1}^{3} \varepsilon^n \phi_n^{(j)}(X_0,X_1,X_2;T_0,T_1,T_2) + o(\varepsilon^4). \tag{14}$$

The short scale $X_0$ and the fast scale $T_0$ denote, respectively, the wavelength and the frequency of the wave. Here, $T_1$ and $T_2$ represent the slow temporal scales of the phase and the amplitude, respectively, whereas the long scales $X_1$ and $X_2$ stand for the spatial modulations of the phase and the amplitude.

For the first order, we can write

$$\eta_1 = \gamma(X_1,X_2;T_1,T_2)\mathrm{e}^{\mathrm{i}(kX_0-\omega T_0)} + \bar{\gamma}(X_1,X_2;T_1,T_2)\mathrm{e}^{-\mathrm{i}(kX_0-\omega T_0)}, \tag{15}$$

where $k$ is the wavenumber, $\omega$ the frequency of the disturbance, $\gamma$ an unknown slowly varying function denoting the amplitude of the propagation wave, which will be determined later, and the bar denotes the complex conjugate. The expansion (13) – (15) is assumed to be uniform for $-\infty < x < \infty$.

To evaluate the boundary conditions (5) – (7), we use the Maclaurin series expansions at $y = 0$ for the quantities involved. Substituting (13) and (14) into (5) – (7), and equating the coefficients of equal powers in $\varepsilon$, we obtain the linear as well as the successive higher-order equations. The hierarchy of the equations for each order can be obtained with the knowledge of the previous orders.

The solution of the first-order problem leads to the dispersion relation

$$\omega^2 = \frac{k[k^2\sigma + g(\rho^{(1)} - \rho^{(2)})]}{(\rho^{(1)}\coth kh_1 + \rho^{(2)}\coth kh_2)}, \tag{16}$$

which is the linear dispersion relation, as obtained earlier by Nayfeh [28], $h_1 \to \infty$ and $h_2 \to \infty$. It is clear that the periodic coefficient of mass and heat transfer has no effect in the first-order problem.

Since we want to investigate the amplitude of the progressive exciting wave, we consider that the right-hand side of (16) is positive and proceeds to higher-order problems. We shall analyze the problem to third-order perturbations only. To construct the amplitude equation, we should solve the boundary value problem to the second-order level of perturbations as well as of the third-order level. In order to obtain valid expansions of the second- and the third-order solutions, the secular terms must be eliminated. The elimination of the secular terms gives the solvability condition. In eliminating the secular terms, we must note that there exist two types of solvability conditions. The first one is obtained when the external frequency $\Omega$ is away from the disturbance frequency $\omega$, i. e. it is the nonresonance case. The second one is the resonance case, which arises when $\Omega$ approaches $2\omega$ or $\omega$.

## 3. The Nonresonance Case

In the nonresonance case, the disturbance frequency $\omega$ is away from the external frequency $\Omega$ or its second harmonic frequency. Accordingly, the solvability condition at the second-order level of perturbations, which is corresponding to the factor $\exp(\pm\mathrm{i}\omega T_0)$, is as obtained earlier by Nayfeh [28]; thus

$$\frac{\partial\gamma}{\partial T_1} + \frac{\mathrm{d}\omega}{\mathrm{d}k}\frac{\partial\gamma}{\partial X_1} = 0. \tag{17}$$

Moreover, the solvability condition, that is imposed from the third-order level of perturbations, is

$$\mathrm{i}\frac{\partial\gamma}{\partial T_2} + \mathrm{i}\frac{\mathrm{d}\omega}{\mathrm{d}k}\frac{\partial\gamma}{\partial X_2} + \frac{1}{2}\frac{\mathrm{d}^2\omega}{\mathrm{d}k^2}\frac{\partial^2\gamma}{\partial X_1^2} + R_0\alpha_0^2\gamma + Q\gamma^2\bar{\gamma} = 0, \tag{18}$$

where

$$R_0 = -\frac{\omega\rho^{*2}}{4(\Omega^2-4\omega^2)}, \tag{19}$$

$$\begin{aligned} Q = &-\frac{kB\omega^2}{2\omega(\rho^{(2)}\coth kh_2+\rho^{(1)}\coth kh_1)} \\ &\cdot\left[-\rho^{(2)}\left(2+\frac{3}{\sinh^2 kh_2}\right)+\rho^{(1)}\left(2+\frac{3}{\sinh^2 kh_1}\right)\right] \\ &+\left[-\frac{3}{2}k^4\sigma+2k\omega^2\left\{\rho^{(2)}\coth kh_2\left(1-\frac{1}{\sinh^2 kh_2}\right)\right.\right. \\ &\left.\left.+\rho^{(1)}\coth kh_1\left(1-\frac{1}{\sinh^2 kh_1}\right)\right\}\right], \end{aligned} \tag{20}$$

$$\begin{aligned} B = &2k\omega^2\left[\left(\rho^{(1)}\coth^2 kh_1-\rho^{(2)}\coth^2 kh_2\right)\right. \\ &\left.+\frac{1}{2}\left(\frac{\rho^{(1)}}{\sinh^2 kh_1}-\frac{\rho^{(2)}}{sinh^2 kh_2}\right)\right] \\ &\cdot\left[4\omega^2\left(\rho^{(1)}\coth 2kh_1+\rho^{(2)}\coth 2kh_2\right)\right. \\ &\left.+\ 2kg\left(\rho^{(2)}-\rho^{(1)}\right)-8k^3\sigma\right]^{-1}, \end{aligned} \tag{21}$$

$$\rho^* = \frac{(\coth kh_1+\coth kh_2)}{(\rho^{(1)}\coth kh_1+\rho^{(2)}\coth kh_2)}.$$

In the light of the Gardner-Morikawa transformation

$$\xi = \varepsilon\left(x-\frac{\mathrm{d}\omega}{\mathrm{d}k}t\right), \quad \tau = \varepsilon^2 t \tag{22}$$

we can rewrite (18) as

$$\mathrm{i}\frac{\partial\gamma}{\partial\tau}+P\frac{\partial^2\gamma}{\partial\xi^2}+R_0\alpha_0^2\gamma+Q\gamma^2\bar{\gamma}=0, \tag{23}$$

where $P=\frac{1}{2}\frac{\mathrm{d}^2\omega}{\mathrm{d}k^2}$. Equation (23) is a standard nonlinear Schrödinger equation which can be used to study the stability behaviour at the nonresonance case. Nayfeh [28] showed that the stability arises as

$$PQ < 0, \tag{24}$$

where he used the following temporal solution for the nonlinear Schrödinger equation (23):

$$\gamma = m_0\exp(\mathrm{i}R_0+\mathrm{i}Qm_0^2)\tau, \tag{25}$$

where $m_0$ is a nonzero constant.

The surface deflection in the nonresonance case is derived as

$$\eta = \varepsilon m_0\cos(kx-\hat{\omega}t)+\varepsilon^2 m_0^2\cos(2kx-2\hat{\omega}t)+\dots, \tag{26}$$

where $\hat{\omega}=\omega-\varepsilon^2(R_0\alpha_0^2+Qm_0^2)$.

## 4. Resonance Mechanisms

It should be noted that the uniformly valid second-order displacement is given by

$$\begin{aligned} \eta_2 = &-2\alpha_2\gamma\bar{\gamma}+\mathrm{i}A\gamma\mathrm{e}^{\mathrm{i}(kX_0-\omega T_0)} \\ &+B_\mathrm{e}\gamma^2\mathrm{e}^{2\mathrm{i}(kX_0-\omega T_0)}+\mathrm{C.C.}, \end{aligned} \tag{27}$$

where

$$\begin{aligned} A = &\frac{\alpha_0\rho^*}{\Omega(\Omega^2-4\omega^2)} \\ &\cdot\left[\omega\Omega\cos\Omega T_0+(\mathrm{i}\Omega^2-2\omega^2)\sin\Omega T_0\right]. \end{aligned} \tag{28}$$

The coefficient $B$ is still the same as defined by (21). Inspection of the second-order displacement (27) reveals that two different small divisor terms do exist. The first one is due to the applied external frequency $\Omega$. When $\Omega\approx 2\omega$, small divisors first appear in the expansion $A$, i. e. in the second-order level of the perturbation. Hence it is called second sub-harmonic resonance case. The second small divisor takes place in $B$, which occurs when

$$(2\omega)^2 = \frac{(2k)^3\sigma+(2k)g(\rho^{(1)}-\rho^{(2)})}{\rho^{(1)}\coth(2k)h_1+\rho^{(2)}\coth(2k)h_2}. \tag{29}$$

Waves that arise because of an interaction between the fundamental waves and their second harmonic ones are known as internal second harmonic resonance. In general, harmonic resonances may exist if $(\omega,k)$ and $(n\omega,nk)$ satisfy the same dispersion relation [12]. When resonance occurs, we find that both the surface distortion and the excited volume pulsation undergo a modulation. At exact resonance, only amplitude modulations occur and the modulations are monotonic functions of time. The volume pulsation increases as it draws energy from the surfaces distortion mode. Near, but not at, resonance, energy exchanges cyclically between the surface and volumetric modes. The oscillations in this case experience both amplitude and phase modulation. The phase modulation, which results in changes in the oscillation frequencies, has previously been observed and studied for oscillations of liquid drops.

In order to study the effect of the time-dependent mass and heat transfer on the wave instability, we proceed to the following resonance cases:

*4.1. The Second Sub-Harmonic Resonance Case*

The second sub-harmonic resonance case arises when $\Omega$ is approaching $2\omega$. In this case we describe the nearness of $\Omega$ to $2\omega$ by introducing the detuning parameter $\delta_1$ defined by

$$\Omega \cong 2\omega + 2\varepsilon\delta_1. \tag{30}$$

At this stage the solvability condition at the second-order level of perturbation is expressed as

$$\frac{\partial\gamma}{\partial T_1} + \frac{\mathrm{d}\omega}{\mathrm{d}k}\frac{\partial\gamma}{\partial X_1} = -\frac{(\Omega-\omega)}{4\omega}\alpha_0\rho^*\bar{\gamma}\mathrm{e}^{-2\mathrm{i}\delta_1 T_1}. \tag{31}$$

Introducing the transformation

$$\gamma(X_1,X_2;T_1T_2) = \lambda(X_1,X_2;T_1,T_2)\mathrm{e}^{-\mathrm{i}\delta_1 T_1}, \tag{32}$$

hence the above solvability condition will reduce to

$$\frac{\partial\lambda}{\partial T_1} + \frac{\mathrm{d}\omega}{\mathrm{d}k}\frac{\partial\lambda}{\partial X_1} = \mathrm{i}\delta_1\lambda - \frac{(\Omega-\omega)}{4\omega}\alpha_0\rho^*\bar{\lambda}. \tag{33}$$

In this case, the second-order displacement (27) can be rewritten if the coefficient $A$ is replaced by

$$\tilde{A} = -\frac{\alpha_0(\Omega+\omega)\rho^*}{2\Omega(\Omega+2\omega)}\mathrm{e}^{-\mathrm{i}\Omega T_0}. \tag{34}$$

In view of this knowledge, the amplitude equation can be constructed from the solvability condition at the third-order perturbations by the help of the second-order level solvability condition (33). The result imposes the following modified nonlinear Schrödinger equation:

$$\mathrm{i}\frac{\partial\lambda}{\partial\tau} + P\frac{\partial^2\lambda}{\partial\xi^2} + \alpha_0\left(R_1\frac{\partial\bar{\gamma}}{\partial\xi} + \mathrm{i}R_3\bar{\lambda}\right) + \alpha_0^2 R_2\lambda + Q\lambda^2\bar{\lambda} = 0. \tag{35}$$

Here the transformation (22) is used. This represents the amplitude equation that governs the behaviour of the wave propagation at the interface and is used to control the stability configuration in the second sub-harmonic resonance case. In the limiting case $\alpha_0 \to 0$, the standard nonlinear Schrödinger equation (35) arises. Such a nonlinear Schrödinger equation has not been investigated before; hence the stability conditions are unknown. In what follows we shall try to derive the stability criteria for the modified Schrödinger equation (35). The coefficients that appear in (35) are

$$\begin{aligned}
R_1 &= \left[\frac{k}{2\omega(\rho^{(1)}\coth kh_1 + \rho^{(2)}\coth kh_2)}\right] \\
&\cdot\left\{\frac{1}{k}\frac{\mathrm{d}\omega}{\mathrm{d}k}\left[-\rho^*(\Omega-\omega)\left(\rho^{(1)}\coth kh_1 + \rho^{(2)}\coth kh_2\right)\right.\right. \\
&\left.\cdot\left(\frac{1}{2\omega} + \frac{(\Omega-\omega)}{\Omega(\Omega-2\omega)}\right) + \frac{1}{2}\left(\coth kh_1 + \coth kh_2\right)\right] \\
&+\frac{(\Omega-\omega)\rho^*}{2k^2}\left[\left(\rho^{(1)}\coth kh_1 + \rho^{(2)}\coth kh_2\right)\right. \\
&\left.+k\left(\frac{\rho^{(1)}h_1}{\sinh^2 kh_1} + \frac{\rho^{(2)}h_2}{\sinh^2 kh^2}\right)\right] + \frac{\rho^*(\Omega-\omega)^3}{2k^2\Omega(\Omega-2\omega)} \\
&\cdot\left[\rho^{(2)}\left(\coth kh_1(1+kh_2\coth kh_2) - kh_2\right)\right. \\
&\left.+\rho^{(1)}\left(\coth kh_1(1+kh_1\coth kh_1) - kh_1\right)\right] \\
&+\frac{k\rho^*\sigma(\Omega-\omega)}{\Omega(\Omega-2\omega)} + \left[\left(kh_1 + \coth kh_1(1+kh_1\coth kh_1)\right)\right. \\
&\left.\left.-\left(kh_2 + \coth kh_2(1+kh_2\coth kh_2)\right)\right]\frac{(\omega-\Omega)}{2k^2}\right\}, \\
R_2 &= -\frac{\rho^*}{4\omega(\rho^{(1)}\coth kh_1 + \rho^{(2)}\coth kh_2)} \\
&\quad\cdot\left\{\frac{\rho^*}{2\omega}\left(\rho^{(1)}\coth hk_1 + \rho^{(2)}\coth hk_2\right)(\Omega-\omega)^2\right. \\
&\quad\cdot\left[\frac{1}{4\omega} + \frac{(\Omega-\omega)}{\Omega(\Omega-2\omega)}\right] + (\coth kh_1 + \coth kh_2) \\
&\quad\left.\cdot\left[-\frac{(\Omega-\omega)}{4\omega} + \frac{2\omega^2}{(\Omega^2-4\omega^2)}\right]\right\}, \\
R_3 &= -\frac{\delta_1(\Omega-\omega)\rho^*}{4\omega^2}.
\end{aligned}$$

*4.2. Stability Analysis for the Modified Nonlinear Schrödinger Equation (35)*

To derive the stability configuration, we follow the Benjamin and Feir [29] and Stuart and DiPrima [30] analysis. Thus, we suppose the following solution for the Schrödinger equation (35):

$$\lambda = m_0\exp\left(\mathrm{i}(R_3/R_1)\xi + \mathrm{i}\alpha_0^2 R_2\tau\right), \tag{36}$$

where the amplitude $m_0$ is given by

$$m_0^2 = \frac{PR_3^2}{QR_1^2}. \tag{37}$$

The amplitude $m_0$ to be real, the following condition is required:

$$PQ > 0. \tag{38}$$

To study the stability criteria of (35) we perturb the solution (36) according to

$$\lambda = (m_0 + m_1(\xi,\tau))\exp\left(\mathrm{i}(R_3/R_1)\xi + \mathrm{i}\alpha_0^2 R_2\tau\right), \quad (39)$$

where $m_1$ is an unknown complex function to be determined. Linearizing in $m_1$, we find that $m_1$ satisfies the equation

$$\begin{aligned} &\mathrm{i}\frac{\partial m_1}{\partial \tau} + P\frac{\partial^2 m_1}{\partial \xi^2} + 2\mathrm{i}P\mu\frac{\partial m_1}{\partial \xi} \\ &\quad + \alpha_0 R_1 \frac{\partial \bar{m}_1}{\partial \xi}\mathrm{e}^{-2\mathrm{i}((R_3/R_1)\xi + \alpha_0^2 R_2 \tau)} \\ &\quad + Qm^2(\bar{m}_1 + m_1) = 0, \end{aligned} \quad (40)$$

where $\bar{m}_1(\xi,\tau)$ is the complex conjugate of $m_1(\xi,\tau)$. Now, we seek the solution of the above equation in the form

$$\begin{aligned} m_1(\xi,\tau) &= a\exp\left(\mathrm{i}(q-(R_3/R_1))\xi + \mathrm{i}(\varpi - \alpha_0^2 R_2)\tau\right) \\ &+ b\exp\left(-\mathrm{i}(q+(R_3/R_1))\xi - \mathrm{i}(\varpi + \alpha_0^2 R_2)\tau\right), \end{aligned} \quad (41)$$

where $a$ and $b$ are complex amplitudes for the modulational wave. The parameters $q$ and $\varpi$ are the modulation wavenumber and frequency, respectively. Substituting the above solution into (36), two coupled equations of $a$ and $b$ are obtained:

$$\begin{aligned} &\big[-(\varpi - \alpha_0^2 R_2) - P(q-(R_3/R_1))^2 \\ &-2P(R_3/R_1)(q-(R_3/R_1)) + 2Qm^2\big]a \\ &+\mathrm{i}\alpha_0 R_1[q-(R_3/R_1)]\bar{b} = 0, \end{aligned} \quad (42)$$

$$\begin{aligned} &\big[(\varpi - \alpha_0^2 R_2) - P(q+(R_3/R_1))^2 \\ &+2P(R_3/R_1)(q+(R_3/R_1)) + 2Qm^2\big]\bar{b} \\ &+\mathrm{i}\alpha_0 R_1[q-(R_3/R_1)]a = 0. \end{aligned} \quad (43)$$

For convenience, (43) has been written as the complex conjugate of the relation, which arises directly. The linear system of (42) and (43) yields the following dispersion relation:

$$\begin{aligned} \varpi^2 &= P^2(q-R_3/R_1)^4 \\ &+ q^2\left[\alpha_0^2(R_1^2 - 2PR_2) - 12P^2R_3^2/R_1^2\right] \\ &+ \left[\alpha_0^4 R_2^2 R_1^4 + \alpha_0^2 R_1^2 R_3^2(6PR_2 - R_1^2) + 16P^2R_3^4\right]/R_1^4. \end{aligned} \quad (44)$$

At this end, the stability constrain requires that

$$\begin{aligned} &P^2(q-R_3/R_1)^4 \\ &+ q^2\left[\alpha_0^2(R_1^2 - 2PR_2) - 12P^2R_3^2/R_1^2\right] \\ &+ \left[\alpha_0^4 R_2^2 R_1^4 + \alpha_0^2 R_1^2 R_3^2(6PR_2 - R_1^2) + 16P^2R_3^4\right]/R_1^4 > 0. \end{aligned} \quad (45)$$

This condition can be satisfied for an arbitrary disturbance $q$, if

$$\alpha_0^2 R_1^2(R_1^2 - 2PR_2) - 12P^2R_3^2 > 0, \quad (46)$$

$$\alpha_0^4 R_2^2 R_1^4 + \alpha_0^2 R_1^2 R_3^2(6PR_2 - R_1^2) + 16P^2R_3^4 > 0. \quad (47)$$

These are the stability criteria for all disturbances $q$. Condition (47) can be written in the form

$$(\alpha_0^2 - \alpha_1^*)(\alpha_0^2 - \alpha_2^*) > 0, \quad (48)$$

where

$$\begin{aligned} \alpha_{1,2}^* = \frac{R_3^2}{2R_2^2 R_1^2}\Big[&-(6PR_2 - R_1^2) \\ &\pm\sqrt{(6PR_2 - R_1^2)^2 - 64P^2R_2^2}\Big]. \end{aligned} \quad (49)$$

Hence, in terms of the amplitude $\alpha_0$, condition (46) can be satisfied as

$$\alpha_0^2 > \alpha^* = \frac{12P^2R_3^2}{R_1^2(R_1^2 - 2PR_2)}, \quad (50)$$

while condition (48) is verified as $\alpha_0^2$ satisfies the inequalities

$$\alpha_0^2 > \alpha_1^* \text{ and } \alpha_0^2 < \alpha_2^*; \quad \alpha_1^* > \alpha_2^*. \quad (51)$$

From the above discussion, the stability at the second harmonic resonance is present as

$$\alpha_0^2 > \alpha^* \text{ and } \alpha_0^2 < \alpha_1^* \text{ or } \alpha_0^2 > \alpha^* \text{ and } \alpha_0^2 < \alpha_2^*.$$

These stability conditions can be obtained numerically.

It is easy to describe the surface deflection in the second resonance case as

$$\begin{aligned} \eta &= 2\varepsilon\frac{R_3}{R_1}\sqrt{\frac{P}{Q}}\cos(\tilde{k}x - \tilde{\omega}t) \\ &+ 2\varepsilon^2\frac{R_3}{R_1}\sqrt{\frac{P}{Q}}\Big[\tilde{A}\sin(\tilde{k}x - (\tilde{\omega} + \Omega)t) \\ &+ B\frac{R_3}{R_1}\sqrt{\frac{P}{Q}}\cos(2\tilde{k}x - 2\tilde{\omega}t)\Big] + \ldots, \end{aligned} \quad (52)$$

where

$$\begin{aligned} &\tilde{k} = k + \varepsilon R_3/R_1 \text{ and} \\ &\tilde{\omega} = \frac{1}{2}\Omega + \varepsilon\frac{R_3}{R_1}\frac{\mathrm{d}\omega}{\mathrm{d}k} - \varepsilon^2 R_2 \alpha_0^2. \end{aligned} \quad (53)$$

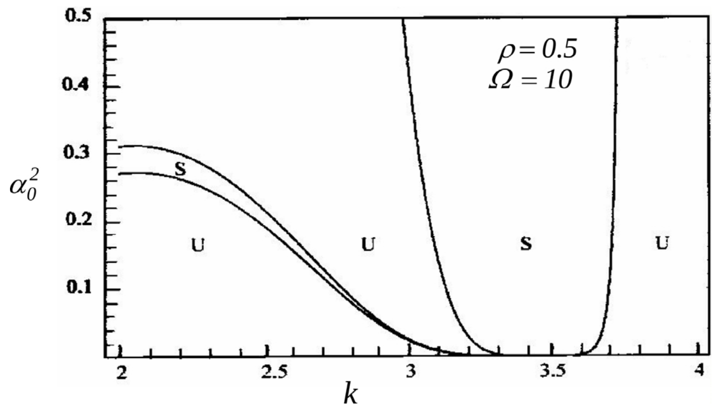


Fig. 1. The stability diagram in the second sub-harmonic resonance case of $\Omega$ near $2\omega$ with $\rho = 0.5$, $h_1 = 1$, $h_2 = 0.5$ and $\Omega = 10$. S, stable region; U, unstable region.

### *4.3. The Third Sub-Harmonic Resonance Case (the Case of $\Omega$ near $\omega$)*

In addition to the terms that produce secular terms in the second-order level there are some terms proportional to the factor $\exp[\pm \mathrm{i}(\Omega - 2\omega)T_0]$ and producing secular terms. To treat this case, we introduce the detuning parameter $\delta_2$, defined according to

$$\Omega = \omega + \varepsilon^2 \delta_2, \tag{54}$$

and hence

$$-\mathrm{i}(\Omega - 2\omega)T = \mathrm{i}\omega T_0 + 2\mathrm{i}\delta_2 T_2. \tag{55}$$

The analysis yields the amplitude equation

$$\begin{aligned} &\mathrm{i}\frac{\partial\gamma}{\partial\tau} + P\frac{\partial^2\gamma}{\partial\xi^2} + R_4\alpha_0^2\bar{\gamma}\mathrm{e}^{-2\mathrm{i}\delta_2\tau} \\ &\quad + R_0\alpha_0^2\gamma + Q\gamma^2\bar{\gamma} = 0, \end{aligned} \tag{56}$$

where

$$R_4 = \frac{(\Omega - \omega)(2\Omega - \omega)}{8\omega\Omega(\Omega - 2\omega)}\rho^{*2}. \tag{57}$$

Equation (56) was investigated by Miles [31] and Umeki [32]. They suggested stationary solutions and studied the stability of the system numerically. To obtain the stability conditions of (56), we follow El-Dib's analysis [19]. Thus the stability conditions are given by

$$Q[\delta_2 + (R_0 + R_4)\alpha_0^2] < 0, \tag{58}$$

$$PQ < 0, \tag{59}$$

$$PR_4\alpha_0^2 > 0. \tag{60}$$

In this case, the surface deflection is given by

$$\begin{aligned} \eta &= 2\varepsilon m^* \cos(kx - \omega^* t) \\ &\quad + 2\varepsilon^2 \left[ \frac{\mathrm{i}\varepsilon\alpha_0\rho^* m^*}{\Omega(\Omega^2 - 4\omega^2)} \big(\omega\Omega\cos\Omega t \right. \\ &\quad + \mathrm{i}(\Omega^2 - 2\omega^2)\sin\Omega\big)\cos(kx - \omega^* t) \\ &\quad \left. + Bm^{*2}\cos 2(kx - \omega^* t) \right] + \ldots, \end{aligned} \tag{61}$$

where

$$\omega^* = \omega + \varepsilon^2\delta_2 \quad \text{and} \quad m^{*2} = -[\delta_2 + (R_0 + R_4)\alpha_0^2]/Q.$$

## 5. Numerical Illustration in the Second Harmonic Resonance Case

In this section, the aim is to determine the numerical profiles of the stability pictures of surface waves propagating through an interface between two superposed fluids. Before performing the numerical calculations for the transition curves in the resonance case, it is convenient to introduce the nondimensional form.

In this dimensionless form the characteristic length is $\lambda = \left(\frac{\sigma}{\rho^{(2)}g}\right)^{1/2}$, and the characteristic time is $\left(\frac{\lambda}{g}\right)^{1/2}$. Other dimensionless quantities are given by $k = \frac{k^*}{\lambda}$, $\rho^{(1)} = \rho\rho^{(2)}$, $h_j = h_j^*\lambda$, $\omega = \omega^*\left(\frac{g}{\lambda}\right)^{1/2}$, $\rho = \rho^{(1)}/\rho^{(2)}$ and $\Omega = \Omega^*\left(\frac{g}{\lambda}\right)^{1/2}$, where the superposed asterisks refer to the dimensionless quantity, from what it will be omitted for simplicity.

In graphing the stability picture in the sub-harmonic resonance case, the numerical computations are made for one of the resonance cases discussed above. The

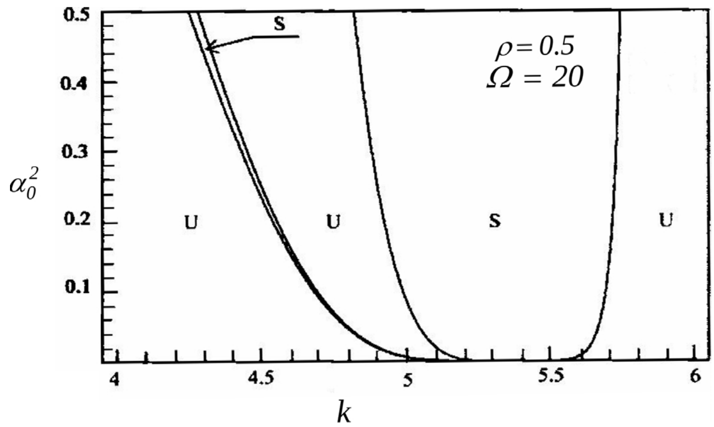


Fig. 2. The same as in Fig. 1, except that $\Omega = 20$.

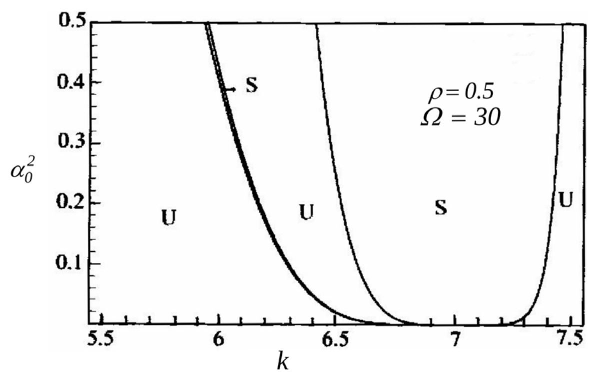


Fig. 3. The same as in Fig. 1, except that $\Omega = 30$.

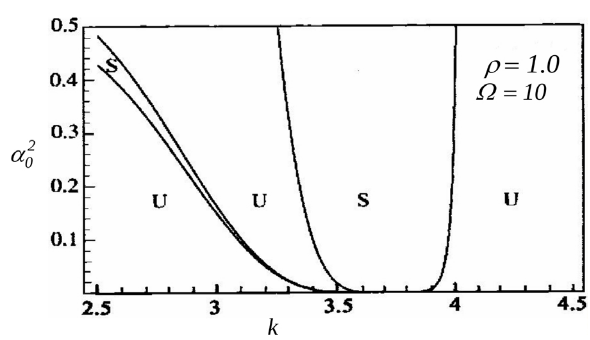


Fig. 4. The same as in Fig. 1, except that $\rho = 1.0$.

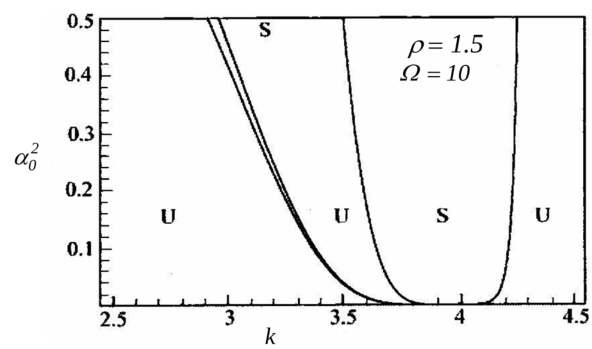


Fig. 5. The same as in Fig. 1, except that $\rho = 1.5$.

resonance case of the heat frequency $\Omega$ approaching twice the disturbance frequency $\omega$ (second subharmonic resonance case) is carried out. Thus, the calculations for the transition curves (49) and (50) are made and displayed in Figures 1 – 5. In these figures, the parameter $\alpha_0^2$ of mass and heat transfer is plotted versus the wavenumber $k$. The stable region is characterized by the symbol S, while the unstable region is labeled by the symbol U. The graph is illustrated in Fig. 1 for a system having $\rho = 0.5$, $h_1 = 1$, $h_2 = 0.5$ and $\Omega = 10$. Inspection of this graph shows that the increase of the amplitude for mass and heat transfer has a destabilizing influence on the stability criteria except for the resonance case. It is found that there are two stable zones bounded by the transition curves and embedded in unstable regions. A narrow stable region associated with a large stable region bounds the sharp resonance case which occurs at the exact case of $\Omega = 2\omega$. This sharp resonance lies at the resonance point having $k = 3.44529$. However, a stabilizing influence is achieved in the resonance case. This stabilizing role is due to the presence of the temperature frequency $\Omega$. The stabilizing influence contrasts to the destabilizing influence of the electric field frequency, see [10, 11, 20] and [21]. To catch the influence of the temperature frequency, we repeated the calculations for Fig. 1 with $\Omega = 20$ instead of $\Omega = 10$; the results are illustrated in Figure 2. Again, Fig. 3 is for increasing the temperature frequency to the value 30. Comparison of Figs. 1, 2 and 3 reveals that an increase in the frequency $\Omega$ yields a shifting of the resonance point towards increasing wavenumber $k$. When $\Omega = 20$, the resonance point is at $k = 5.355794$, while for $\Omega = 30$, it lies at $k = 6.989165$. Associated with shifting of the resonance point, there is an increasing width of the stable zone in the resonance region. This shows stabilizing for increasing the temperature frequency. It is clear that the frequency $\Omega$ destabilizes the amplitude $\alpha_0$. Elhefnawy and Radwan [33] have demonstrated that the mass and heat transfer have a destabilizing influence on the system.

In order to examine the variation of the density ratio on the stability behaviour, we repeated the calculations of Fig. 1 taking $\rho = 1.0$ and $\rho = 1.5$. The results are displayed in Fig. 4 and 5, respectively. Comparison of Figs. 1, 4 and 5 shows that the increase in $\rho$ affects the narrow stable region, in which a destabilizing role is found. On the other hand, the increase in $\rho$ leads to a slight shift of the resonance point in the direction of increasing $k$. It is found that the resonance point lies at $k = 3.71515$ when $\rho = 1.0$, and at $k = 3.94803$ when $\rho = 1.5$.


[1] G. E. Fortescue and J. R. A. Pearson, Chem. Eng. Sci. **22**, 1163 (1967).
[2] M. Rashidi, Int. J. Heat Mass Transfer **34**, 1799 (1991).
[3] R. P. Salazar and E. Marshall, Int. J. Multiphase Flow **4**, 487 (1978).
[4] S. Komori, R. Nagaosa, and Y. J. Murakami, J. Fluid Mech. **249**, 161 (1993).
[5] D. Y. Hsieh, Trans. ASME D **94**, 156 (1972).
[6] A. Korichi and L. Oufer, Int. J. Heat Fluid Flow **28**, 1003 (2007).
[7] D. Y. Hsieh, Phys. Fluids **21**, 745 (1978).
[8] D. Y. Hsieh, Phys. Fluids **22**, 1435 (1979).
[9] A. A. Mohamed, A. R. F. Elhefnawy, and Y. D. Mahmoud, Physica A **195**, 74 (1993).
[10] A. A. Mohamed, A. R. F. Elhefnawy, and Y. D. Mahmoud, Can. J. Phys. **72**, 537 (1994).
[11] A. R. F. Elhefnawy and G. M. Moatimid, Phys. Scr. **50**, 258 (1994).
[12] A. H. Nayfeh, Perturbations Methods, Wiley, New York 1973.
[13] Y. O. El-Dib, J. Phys. A: Math. Gen. **30**, 3585 (1997).
[14] A. A. Mohamed, E. F. Elshehawey, and Y. O. El-Dib, J. Colloid Interface Sci. **207**, 54 (1998).
[15] G. M. Moatimid, J. Phys. D **27**, 1390 (1994).
[16] Y. O. El-Dib, Chaos, Solitons and Fractals **5**, 1007 (1995).
[17] Y. O. El-Dib, Appl. Math. Lett.**7**, 89 (1994).
[18] Y. O. El-Dib, Chaos, Solitons and Fractals **11**, 1773 (2000).
[19] Y. O. El-Dib, Nonlinear Dyn. **24**, 399 (2001).
[20] Y. O. El-Dib, in: Advances in Plasma Physics Research, Vol. 4, Chapter 3 (Ed. F. Gerard), Nova Science Publishers, Inc., New York 2003.
[21] Y. O. El-Dib, IMA J. Appl. Math. **55**, 97 (1995).
[22] Y. O. El-Dib, Can. J. Phys. **72**, 578 (1994).
[23] A. R. F. Elhefnawy, Y. O. El-Dib, and Y. D. Mahmoud, Int. J. Theor. Phys. **36**, 2079 (1997).
[24] G. M. Moatimid, J. Colloid Int. Sci. **250**, 108 (2002).
[25] G. M. Moatimid, Phys. Scr. **65**, 490 (2002).
[26] G. M. Moatimid, J. Colloid Int. Sci. **259**, 186 (2003).
[27] Y. D. Mahmoud, J. Mag. Mag. Mat. **195**, 779 (1999).
[28] A. H. Nayfeh, J. Appl. Mech. **98**, 584 (1976).
[29] T. B. Benjamin and T. E. Feir, J. Fluid Mech. **27**, 417 (1967).
[30] J. T. Stuart and R. C. DiPrima, Proc. R. Soc. London A **362**, 27 (1978).
[31] J. W. Miles, J. Fluid Mech. **148**, 451 (1984).
[32] M. J. Umeki, J. Phys. Soc. Jpn. **60**, 146 (1991).
[33] A. R. F. Elhefnawy and A. E. Radwan, Physica A **190**, 330, (1992).